Towards Automated Power Line Corridor Monitoring Using Advanced Aircraft Control and Multi-source Feature Fusion

Zhengrong Li [1,2], Troy S. Bruggemann [1], Jason J. Ford [1], Luis Mejias [1], Yuee Liu [1]

[1] Australian Research Centre for Aerospace Automation, Queensland University of Technology, Boronia Road, Eagle Farm, QLD 4009, Australia

[2] ROAMES, Ergon Energy, Mary Street, Brisbane, QLD 4000, Australia

ABSTRACT

The conventional manual power line corridor inspection processes that are used by most energy utilities are labor-intensive, time consuming and expensive. Remote sensing technologies represent an attractive and cost-effective alternative approach to these monitoring activities. This paper presents a comprehensive investigation into automated remote sensing based power line corridor monitoring, focusing on recent innovations in the area of increased automation of fixed-wing platforms for aerial data collection, and automated data processing for object recognition using a feature fusion process. Airborne automation is achieved by using a novel approach that provides improved lateral control for tracking corridors and automatic real-time dynamic turning for flying between corridor segments, we call this approach PTAGS. Improved object recognition is achieved by fusing information from multi-sensor (LiDAR and imagery) data and multiple visual feature descriptors (color and texture). The results from our experiments and field survey illustrate the effectiveness of the proposed aircraft control and feature fusion approaches.

Keywords: Power Line Corridor Monitoring, Vegetation Management, Automatic Aircraft Control, Multi-source Data Fusion, LiDAR, Multi-spectral Imagery, Kernel PCA, Image Classification.

1. INTRODUCTION

There is no doubt about the increased reliance that modern societies have on electricity. Electrical companies are under continuous and significant pressure to ensure reliable supply and distribution of electricity. Whilst trees, shrubs and other vegetation are of remarkable importance to the environment and our daily life, inappropriate vegetation around power lines can represent a significant risk to public safety and is one of the main causes of power outages. It is commonly known that trees falling across power lines are the largest cause of power failures, causing widespread power outages and bushfires (Ituen and Sohn 2010; Mills, Gerardo, Li et al. 2010). Hence, it is not surprising that power line corridor vegetation management procedures have become a significant maintenance cost for electrical companies. For example, Ergon Energy, Australia's largest geographic footprint energy distributor, currently spends over $80 million a year inspecting and managing vegetation encroachments on power lines. Correct and efficient vegetation management not only reduces the overall cost but also aids in continuous electricity supply by preventing damage to power lines through removal of intrusive trees. Ineffective procedures can result in the loss of reliability in electricity transmission, produce serious hazards and expose electrical companies to significant financial penalties.

A power line corridor describes the strip of land upon which utility companies construct their electrical infrastructure. Monitoring power line corridors is crucial for the reliability of electricity transmission. Trees and shrubs often create obstructions in corridors and pose risks to power lines, and therefore utility companies need to scrutinize where and how trees grow in or close to power line corridors (Ituen and Sohn 2010). In urban areas, vegetation encroachment is less serious than in rural areas as access is much easier and prompt maintenance can be achieved. Moreover, local councils and private land owners regularly maintain their trees facilitating the overall maintenance process. However, in rural areas, inspection maintenance becomes difficult due to limited access and large distances to cover. In these areas, traditional calendar-based tree trimming is often a strategy used by energy distributors. Other short-term strategies might be to identify and remove nearby objects (i.e. buildings and vegetation) found near power lines. More generally, the risk of manmade structures can be controlled through building regulations. However, vegetation grows naturally and particularly in rural areas, the growth of vegetation is unmanaged. Strong winds and storms can bring branches or even entire trees into contact with power lines. Unmanaged vegetation

can also grow up into power lines and cause bushfires. Unfortunately, vegetation management over large powerline networks is cumbersome and expensive. To manage the tradeoff between safety and cost, utility companies often introduce a regular maintenance cycle (e.g. say once every 5 years). This strategy assumes that once inspected, properly maintained vegetation can be assumed to remain separated from the power line infrastructure until the maintenance cycle is repeated 5 years later. However, trees often grow unexpectedly during the period between maintenance due to inaccurate vegetation growth modeling and climate changes. For example, the Australian state of Queensland is subject to extreme weather conditions, ranging from drought to cyclones. Moreover, Queensland can suffer extended periods of dry conditions which significantly increase the risk of fire. Strong winds and waterlogged ground can result in trees falling across, and bringing down power lines, especially when inappropriate vegetation species have grown too close to power lines. Conventional vegetation management strategies only consider the direct clearance of a small number of trees within tight corridors below the power line infrastructure, whilst the growth of nearby and potentially troublesome vegetation that is slightly outside the corridor is often neglected. Whilst indiscriminate removal of all vegetation within a power line corridor is neither cost-effective nor eco-friendly, better longer term strategies can be achieved by improved monitoring and modeling the growth of all vegetation surrounding power line infrastructure.

The subjective nature of conventional maintenance strategies often result in some zones being trimmed more frequently than required, or conversely, some zones not being trimmed often enough. Remote sensing technologies represent an attractive and potentially automated solution for power line corridor monitoring activities. Recent efforts toward remote sensing based methods include improved data collection using satellite sensors (Beltrame, Jardini, acbsen et al. 2007; Kobayashi, Karady, Heydt et al. 2009), an airborne stereo vision system (Sun, Jones, Wu et al. 2006), and unmanned aerial vehicles (UAVs) (Jones, Golightly, Roberts et al. 2005; Li, Liu, Walker et al. 2010). Recently airborne laser scanning has attracted particular attention in power line corridor monitoring problem due to the possibility of achieving three dimensional models of infrastructure (Chaput 2008; Lu and Kieloch 2008; Jwa, Sohn and Kim 2009). Many utility companies and researchers, if not most, use commercial data and software but also generate algorithms tailored for their needs. However, there are some critical issues to be addressed regarding automated data collection and processing over complicated power line networks. For example, the quality of collected data has much to do with aircraft platform stability. The complex nature of navigating

aircraft over extensive amounts of power line networks calls for an increased level of flight automation. To increase the reliability of the information extraction from remote sensing data, combining the complementary information derived from multi-source data can be very useful. The effective fusion of multi-source data provides the opportunity for more robust operational performance and decision making in power line corridor monitoring

This paper begins in Section 2 with a survey of the remote sensing based power line corridor monitoring. We then detail two important aspects of the power line corridor monitoring problem: advanced aircraft control for power line corridor monitoring, and multi-sensor data fusion for vegetation classification. For this purpose, we first summarize our receding virtual waypoint and precision guidance tracking approach reported previously in (Bruggemann, Ford and Walker 2010). We then summarize our automated data processing work reported previously in (Li, Liu, Walker et al. 2010; Mills, Gerardo, Li et al. 2010; Li, Hayward, Walker et al. 2011). In Section 3, we present some new flight tests results that evaluate the ability of the inspection aircraft to maintain a LiDAR swath width over the features of interest. Then, a new automated aircraft behavior for maneuvering capability at power line corridor corners is described and flight test results presented. In Section 4, new approaches and results for the combined use of LiDAR and multi-spectral image data, as well as the fusion of multiple visual feature descriptors are presented. The paper ends in Section 5 by presenting some conclusions drawn from the lessons we learnt during our 3-year power line corridor monitoring project.

2. TECHNOLOGY OVERVIEW

2.1. Power Line Corridor Monitoring Using Aerial Remote Sensing

Ergon Energy has a long-term strategy of managing vegetation according to different species; species can be generally categorized as either desirable or undesirable species. Species with fast growth rates and that also have the potential to reach a mature height of more than four meters are defined as undesirable species. These undesirable species often pose high risks to electrical infrastructure and therefore should be identified and removed. It is also worth mentioning that a reasonable long-term maintenance strategy is to encourage low-growing trees or shrubs because they are expected to compete with tall growing species and deprive the taller trees of light and nutrients. These low growing species, along with the rare and endangered species, are defined as desirable species that should be managed differently.

The need to manage risk motivates the collection of data over power line corridors and the identification of objects of interest in order to assess the risk levels and guide the field workers for vegetation clearance in the corridors. Remote sensing represents a particularly attractive solution for power line corridor monitoring. Actually, aerial vehicles have been intensively used in power line inspection for a long period. One present practice is to fly helicopters/airplanes along the corridor and try to identify dangerous trees and assess the condition of overhead lines assets by visual observation. Such visual inspection is time consuming and labor intensive. The advances in sensor technologies and intelligent computing techniques provide the opportunity to move from traditional vegetation management strategies to more automated, accurate and cost-effective solutions.

2.1.1. Remote Sensing Platforms

Satellites and aircraft are the most widely used platforms for remote sensing in earth observing data collection. Current satellite sensors are not the best choice for monitoring power line corridors due to two critical limitations: the unfavorable revisit time and lack of choices in optimum spatial and spectral resolutions. At the most practical level, most collections of data gathered from satellites are available only on predetermined schedules, and even those with an "on-demand" capability are also limited by their orbits and the demands of other users. In contrast, airborne data collection offers a much greater level of flexibility. Another advantage of an airborne platform is that different sensor payloads can be easily fitted, while the sensors launched on a satellite are rarely changeable. As a consequence, airborne systems can be regularly upgraded as sensor technology advances. Improvements to sensors include systems with higher spectral and spatial resolution, and advanced microwave or LiDAR sensors. In addition, higher spatial resolutions are easier to obtain from airborne platforms, due to their low altitude. A limitation which impedes large-scale airborne remote sensing applications is that the traditional piloted airborne platforms involve high operational costs. Moreover, using piloted aircraft for power line inspection will place the pilots at a greater level of risk. Many airborne LiDAR systems, if not most, use helicopter platforms (Ituen and Sohn 2010). Although flying LiDAR with a rotorcraft has some advantages over fixed-wing aircraft where tight turns are required, a fixed-wing aircraft has advantages over rotorcraft in terms of cost per kilometre surveyed in the large-scale aerial inspection tasks that we are considering in this paper.

Remote sensors mounted on unmanned aerial vehicles (UAVs) could fill this capability gap, providing a cheap and flexible way to gather spatial data from power line corridors which can also

meet the requirements of spatial, spectral, and temporal resolutions. Recent developments in the aerial vehicles themselves and associated sensing systems make UAV platforms increasingly attractive for both research and operational mapping (Berni, Zarco-Tejada, Suárez et al. 2009; Gurtner, Greer, Glassock et al. 2009). One of the main barriers to using UAVs is their inability to carry power-demanding and heavy payloads. LiDAR systems are usually too heavy for small/medium sized UAV platforms. This UAV limitation may be overcome in the near future as there are already small LiDAR systems in the market suitable for UAVs. However, the performance of these units in terms of the quality of data collected is currently well away from their full-sized counterparts and more development is required. Another key barrier to using UAV is the aviation regulatory issues associated with using UAV outside of visual range of an operator. However, if both these barriers can be addressed, the combination of small LiDAR type systems and advanced UAVs might represent a powerful aerial inspection technology.

The above mentioned limitations of current UAV technology motivate consideration of manned semi-autonomous systems as a technological step from manually piloted inspection towards fully autonomous operations. Manned semi-autonomous systems would provide increased automation in the aerial survey task but also allow the pilot to remain onboard to monitor and provide human control and oversight of the flight. Manned semi-autonomous operation has advantages over the current manually piloted approach such as reducing the crewing requirements (pilot only, instead of sensor operator and pilot), and allowing a pilot without specialized skills in flying above powerlines to safely and routinely conduct successful aerial surveys. Safety could also be improved by reducing pilot fatigue and by allowing the pilot to focus upon important aircraft safety-of-operation tasks such as the “see-and-avoid” function.

2.1.2. Automated Data Processing

There are two kinds of remote sensing: passive remote sensing and active remote sensing. Passive sensors detect natural radiation that is emitted or reflected by the object or surrounding area being observed. Reflected sunlight is the most common source of radiation measured by passive sensors. Optical remote sensing images such as satellite and airborne multi-spectral imagery are collected from passive sensors. The spatial resolution and spectral resolution are the two most important characteristics of optical remote sensing imagery. Spatial resolution commonly referred to as “pixel size” in digital images, has a close relationship with the information content that can be extracted from the image; however, higher spatial resolution is not always beneficial. In many sensor

processing problems, images with a spatial resolution near the size of the object of interest are often preferred (Lefsky and Cohen 2003). Spectral resolution is the richness of spectral information in optical remote sensing imagery. Different materials reflect and absorb differently at different wavelengths. Spectral features are the specific combination of reflected and absorbed electromagnetic radiation at varying wavelengths which can uniquely identify an object. For example, near-infrared (NIR) wavelengths have been successful applied to estimating vegetation biophysical properties (Rautiainen 2005). Active sensors, on the other hand, emit energy in order to scan objects and areas whereupon a passive sensor then detects and measures the radiation that is reflected or backscattered from the target. Light detection and ranging (LiDAR) is an example of active remote sensing in which the properties of returned scattered light are used to find range or other information of a distant target. Traditionally, the primary use of LiDAR data is to obtain altitude data and generate digital terrain models (DTM). In recent years, however, the range of applications in which laser scanning can be used has greatly broadened. With the advancement of sensor technology, the achievable resolution of point clouds makes it possible to map individual trees and power lines from airborne laser scanning data.

As may already be evident from the previous section, aerial remote sensing represents an attractive solution for power line corridor mapping. Compared to corridor mapping, automated and intelligent information extraction from remotely sensed data is even more challenging. One special need for power line corridor monitoring is to automatically detect the objects of interest for further interpretation and decision making (major objects of interest include power line assets and vegetation). Automated data processing aims to automatically detect these objects from aerial imagery, and tries to extract more specific information such as vegetation species and height information.

Risk assessment of power lines and adjacent trees is meaningful only when power lines and trees can be detected. A number of papers have been published on power line detection during the past a few years, both from 2D imagery and 3D LiDAR point cloud data. A straight line can approximate a power line segment in aerial images. Therefore, some classic line detection algorithms like the Hough transform may be used to detect power lines in images. Yan et al. employed Radon transform to extract line segments of the power lines, followed by a grouping method to link each segment and a Kalman filter to connect the segments into an entire line (Yan, Li, Zhou et al. 2007). Li et al. developed a filter based on a simplified pulse coupled neural network model (Li, Liu,

Walker et al. 2010). This filter can simultaneously remove the background noise as well as generate edge maps. After that, an improved Hough transform is used by performing knowledge-based line clustering in Hough space to refine the detection results. The accuracy of 2D image based power line detection algorithm depends on the quality of the image. Low spatial resolution and motion blur are the two major causes of the failure of the power line detection algorithms. LiDAR is more popular for power line survey than image-based approaches because it can provide high density point cloud data and does not rely on illumination conditions. LiDAR can more effectively generate accurate elevation and terrain models, which can also help to remove terrain points and other similar linear features (e.g. fences). Moreover, the 3D nature of LiDAR data makes it possible to model the sag of lines, which is also crucial for the maintenance of electrical infrastructure. For 3D LiDAR point cloud data, line detection can be conducted either by clustering similar features in a voxel (Jwa, Sohn and Kim 2009) or mapping 3D data to two 2D planes (horizontal and vertical) and then roughly detecting the power line points in the horizontal plane and reconstructing the catenary curve in the vertical plane (Liu, Li, Hayward et al. 2009). No matter which method is used, prior removal of non-powerline points (e.g. terrain, tree and building) will always be helpful to reduce the false positive rate in power line detection.

Tree detection from remote sensing imagery is well researched, particularly in the context of forest and plantation management (Pouliot, King, Bell et al. 2002; Mallinis, Koutsias, Tsakiri-Strati et al. 2008). According to our literature review, image based tree detection methods can be broadly categorized as either local maxima/minima, template matching, region growing, or edge detection approaches (Li, Hayward, Zhang et al. 2008). As the most widely used tree detection method, the local maxima/minima approach uses the following assumption: the radiometric properties of a tree can be described through a mountainous landscape in which peaks are approximate crown apexes, and surrounding valleys represent the space between crowns or where crowns overlap or touch (Pouliot, King and Pitt 2005). However, this assumption is not always true. In some real situations, multiple trees touch closely and have no distinct dark boundary between tree crowns. Research indicates that in this case template matching gives better results, however it is very time consuming (Erikson and Olofsson 2005). Another drawback of the local maxima/minima approach is the initial assumptions about crown size and shape, and the relative inflexibility of the model to accommodate irregular crown form. Considering the spectral properties of vegetation, particular near-infrared band, can be very helpful to detect trees. Li et al. employed a simplified pulse-coupled neural

network (PCNN) that uses spectral features as input, post-processed using morphological reconstruction (Li, Hayward, Zhang et al. 2009). The algorithm has been shown to outperform both JSEG (Deng and Manjunath 2001) and TreeAnalysis (Erikson 2003) in tree crown segmentation, but the primary error source is the under-segmentation of tree clusters due to the crown overlap. LiDAR system can measure both vertical and horizontal structures of object, which make it a good means for detecting individual trees and estimating tree parameters. Many LiDAR based tree detection algorithms borrow the idea from image based methods. Leckie et al. applied the valley-following method (Leckie, Gougeon, Hill et al. 2003), and Kwak et al. segmented individual trees from LiDAR data using extended maxima transformation of the morphological image-analysis method (Kwak, Lee, Lee et al. 2007). Despite the benefit of 3D information in tree segmentation, the lack of spectral and texture information makes it hard to derive more detailed vegetation information (e.g. biophysical properties and species) only from LiDAR data. Combination of LiDAR data and optical imagery is considered to be a very promising solution.

2.2. Control of Airborne Platform

Maintaining stability and control of a fixed-wing airborne platform above a powerline corridor is necessary for reliable data capture of ground assets and features such as powerlines and vegetation. To achieve data capture objectives with a body-fixed downward pointing LiDAR or camera, the aircraft must maintain an accurate track over the powerline corridor, with minimal lateral position and angular heading deviation from the desired flight path over the line. The lateral position deviation is referred to as cross-track error and is a key parameter which the controller attempts to minimise. At the same time, platform orientation must be controlled and stabilized since excessive aircraft bank angle may result in parts of the corridor being missed or poor captured data quality (Nelson, Barber, McLain et al. 2006; Bruggemann, Ford and Walker 2010; Holt and Beard 2010)

2.2.1. Limitations of Current Aerial Survey Industry Practices and Technologies for Inspecting Powerline Corridors

Currently in the aerial survey industry, platform stability and tracking is typically maintained by manual pilot control with operator assistance. Pilots are required to concentrate upon a flight display for extended periods of time during inspection must be allowed regular breaks for rest and recovery. A representative diagram of this approach is given in Figure 2. However the powerline inspection task can involve flying extensive amounts of powerline corridor on a routine basis. For example

Ergon Energy's network in Queensland, Australia consists of 150,000 km of powerline and could require 4000 hours or more flying time to inspect the whole network. Flying aircraft at low altitude over powerlines for up to 4 or 5 hours a time is a tedious and potentially dangerous task under manual piloted control. We argue that improved safety of airborne operations and an increased reliability of data capture may be achieved through the increased use of flight automation for inspection tasks.

However, our study of current autopilots and GPS navigators showed that these existing technological solutions are not designed for controlling an aircraft to track powerlines - they are designed chiefly for routine navigation including waypoint to waypoint navigation and conducting holding patterns and procedure turns. Further, standard autopilots and GPS navigators typically lack the configurability and tuneability required to allow them to perform in a suitable way for powerline corridor inspection. Unlike waypoint to waypoint navigation, tracking powerline corridors for inspection requires both aircraft translational and rotational motion to be controlled (Bruggemann, Ford and Walker 2010). It should be clear from consideration of the powerline network to be flown (Figure 1) that, from an automatic control point of view, a different solution is required to that provided by standard autopilots and navigators, because:

- The powerline network consists of many large and sudden changes in line direction as well as short spacing between lines sections. This presents automatic control challenges such as how to maintain accurate position over the line, yet also limit and control aircraft orientation (e.g. bank angle) such that no sections of the corridor are missed (Bruggemann, Ford and Walker 2010). Also, terrain variations and aircraft altitude and speed need to be considered.
- A very large number of waypoints are required to specify a powerline network under inspection. This presents challenges in both waypoint database management and flight planning. For example, Ergon's electrical distribution in Queensland is described by approximately 1 million waypoints.
- Typically, the total width of a specified powerline corridor must be inspected (not just the powerline itself) and this requirement necessitates consideration and monitoring of aircraft orientation and the sensor footprint on the ground.
- Automatic turn re-planning around powerline corridor segments (in cases of excessive cross-track error or bank angle requiring a go-around maneuver) is also advantageous for reliability of data capture.

New automatic control technology could allow improved safety by removing the need for the pilot to manually maintain track and orientation over the line and allowing the pilot to focus upon operating the aircraft and situational awareness. It could also facilitate single crew operations that do not require an additional operator to assist the pilot.

Past research has focused on the problem of automatic control of airborne platforms for the purpose of aerial inspection of linear assets such as rivers, roads, pipelines and powerlines (Frew, McGee, Kim et al. 2004; Rathinam, Kim, Soghikian et al. 2005; Egbert and Beard 2007; Holt and Beard 2010). Early studies discovered that simple PID-based control loops can lead to poor cross-track error performance due to GPS derived tracking errors (Niculescu 2001; Frew, McGee, Kim et al. 2004). Hence, nonlinear controllers based on minimization of heading or heading error rate were proposed (Niculescu 2001; Frew, McGee, Kim et al. 2004). Alternative line tracking strategies related to proportional navigation type guidance laws such as biased proportional navigation (Holt and Beard 2010) and precision guidance (Bruggemann, Ford and Walker 2010) have also been proposed. Vector field and Lyapunov based approaches have also been proposed for more general path tracking problems with UAVs (Ren and Beard 2004; Nelson, Barber, McLain et al. 2006).

The past control literature acknowledges the problem of maintaining features of interest within the sensor field of view; however, the issues associated with tracking powerline corridors and their impact on LiDAR swath width have not been well studied. The swath width of a LiDAR is the across-track distance that is mapped while on a survey line (Costa, Battista and Pittman 2009). Swath width depends upon LiDAR scan angle and also aircraft height above terrain. In tracking powerline corridors, it is desired to capture a corridor region. The swath width is an important parameter in survey applications as it needs to be wide enough such that the LiDAR scanning beam covers the complete width of the corridor region to be surveyed, yet narrow enough such that the point cloud density is dense enough to capture specific (and possibly thin) features of interest such as individual powerlines. Since LiDAR data files are large, narrow swath width also has advantages in terms of reducing the amount of data stored during a survey flight. Integrated system design, automatic guidance, maneuver and control solutions for an aircraft tracking linear infrastructure has already been investigated in (Bruggemann, Ford and Walker 2010). However, the impacts on LiDAR swath width when tracking powerline corridors and the ability to conduct automatic turns around powerline corridors were not investigated in this earlier work. For this purpose an evolved

prototype of the architecture presented in (Bruggemann, Ford and Walker 2010) called the Powerline Tracking Automatic Guidance System (PTAGS) was developed as described next.

2.2.2. Powerline Tracking Automatic Guidance System (PTAGS)

The Powerline Tracking Automatic Guidance System (PTAGS) provides improved lateral control for tracking corridors and automatic real-time dynamic turning for flying between corridor segments. A diagram of the system architecture is given in Figure 3. PTAGS takes waypoints describing the powerline corridors as input from a flight and waypoint management system and commands a standard aircraft autopilot, whilst considering both translational and rotational motion with respect to the corridor. A key feature of this approach is the feedback loop from aircraft performance (aircraft position and orientation with respect to the powerline corridor as measured by onboard navigation systems) to PTAGS which then utilizes new automated guidance, maneuver and control algorithms to command the aircraft autopilot. It also includes automatic decision-making which enables the autopilot to plan and fly turns that incorporates available knowledge at the time such as LiDAR swath width, aircraft airspeed and roll angle. Dynamic turn re-planning ("go-around") capability in the case of missed data capture or unacceptable cross-track or roll angle tolerances is also implemented.

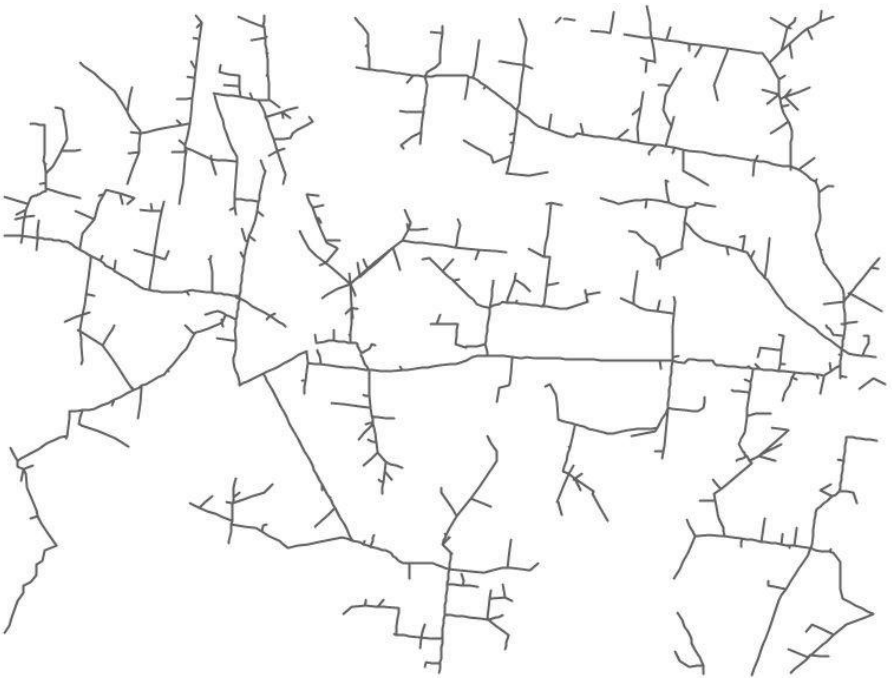

Figure 1 A 20 km by 15 km area of powerline network (black lines). The distribution, size and orientation of lines indicate challenges for automated guidance and control of a fixed-wing airborne

platform. Large and sudden changes in line direction and short spaces between lines sections require specialized control techniques.

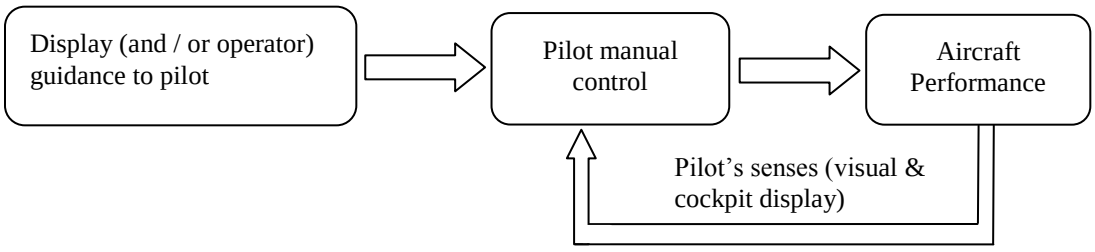

Figure 2 Manual control of inspection aircraft (current industry practice).

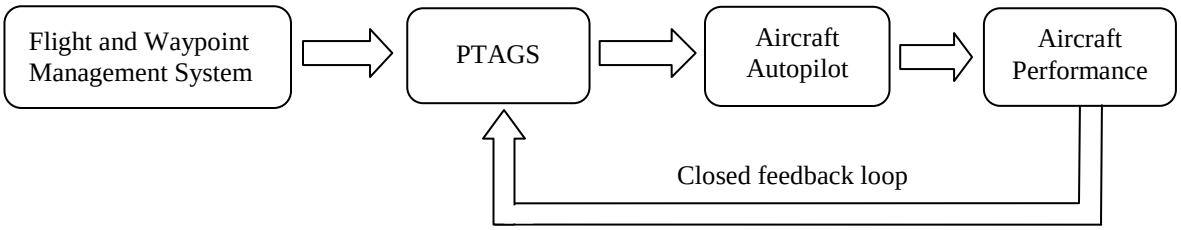

Figure 3 Automatic control of inspection aircraft with PTAGS

The control system architecture of PTAGS is given below (Figure 4) as already presented in (Bruggemann, Ford and Walker 2010). The key functions of PTAGS are the Receding Virtual Waypoint (RVWP), Guidance and Maneuever Selection which send roll guidance commands to the aircraft autopilot. The architecture is decomposed and approximately sorted according to the time scales of the dynamics handled within each loop. The outer loop (guidance) corresponds to slower features of the dynamics (translational motion), whilst the inner loop (autopilot) controls the faster dynamics (rotational motion). This decomposition allows the inner autopilot loop to be handled by an already certified commercial autopilot; the use of certified autopilots simplifies the process for certification of the overall developed inspection solution. In fact, we have safely conducted flight experimentation with a Cessna 172 aircraft for the past two years, with appropriate approval by the regulators. This decomposition also allows platform specific issues to be contained within one loop such that the design of the outer loops is less dependent upon platform specifics, allowing re-use on different aircraft platforms.

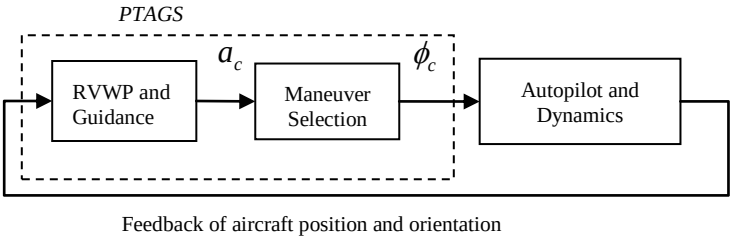

Figure 4 Control system architecture of PTAGS.

The trajectory planning and guidance functions are indicated by the Receding Virtual Waypoint (RVWP) and Guidance block on Figure 4. The RVWP is specified as a point on the infrastructure at some look ahead distance ahead of the aircraft's current location, and the point moves along the infrastructure as the aircraft moves along. A feature of this approach is the avoidance of discontinuities in the planned flight path (due to corners where powerline segments join) which results in "cutting across corners" behavior. When using a RVWP approach to describe the reference trajectory, the lateral stability of the platform depends upon characteristics of the autopilot response and the look ahead distance selected.

The guidance function in PTAGS utilizes a precision guidance law which commands a lateral acceleration a_c to minimize the track error between desired flight trajectory and current aircraft location. The lateral acceleration commands are calculated from current aircraft location, current receding virtual waypoint location, and the heading direction of the powerline infrastructure to be tracked. Further details are published in (Bruggemann, Ford and Walker 2010).

The maneuver selection block includes switching logic between control for "on survey" and "off survey" tasks. On survey is when the LiDAR system will be switched on and collecting data, over the powerline corridor infrastructure. In this case the powerline corridor itself describes straight line piecewise linear paths to be tracked and defines the reference trajectory for the RVWP. But there are also "off survey" periods where the aircraft is conducting maneuvers such as steady turns to align itself in preparation for the next "on survey" inspection leg. In "off survey" periods a curved reference trajectory for conducting a turning maneuver is constructed based upon Dubins paths (Chitsaz and LaValle 2007), and the receding virtual waypoint moves along this curved path with tracking provided by the precision guidance law, to achieve an automatic turning control. Roll

commands ϕ_c are then sent to the autopilot, which have been determined from lateral acceleration commands a_c using a simple kinematic bank turn model as described in (Bruggemann, Ford and Walker 2010). Studies of the performance of PTAGS in "off survey" mode tracking a curved reference trajectory and impacts of the "on survey" line tracking mode on LiDAR swath width will be presented in Section 3.

2.3. Multi-source Feature Fusion for Improved Vegetation Classification

LiDAR is an effective sensor for 3D information acquisition and has great potential to assist vegetation management in power line corridors. However, due to the variations of point density and lack of spectral information, it is often hard to achieve robust tree detection results from only LiDAR data. Distinct spectral signatures in red and near-infrared bands have been successfully used to discriminate vegetation and non-vegetation (Li, Hayward, Zhang et al. 2009). However, grass, low vegetation is hard to be discriminated from trees as they present very similar colors and even textures. A better solution is to combine multispectral images and LiDAR data to improve tree detection and segmentation.

As discussed in section 2.1, the species information is valuable to model the growth of vegetation and discriminate desirable and undesirable tree species. Tree species classification from remote sensing data has been intensively studied in forest management (Sugumaran, Pavuluri and Zerr 2003; Holmgren, Persson and Söderman 2008; Breidenbach, Næsset, Lien et al. 2010). However, successful classification is mostly seen at forest stand level or individual trees with different genus (e.g. coniferous or deciduous species) because they look obviously different in visual appearance. Detailed individual tree species is often hard to discriminate due to their similarity in visual features, even for human expert interpretation from imagery or field survey. We borrow the idea commonly used in human face recognition and try to improve tree species classification by selecting more discriminative visual feature descriptors. A feature fusion method is developed by combing color and texture feature descriptors using kernel PCA and maximum likelihood based intrinsic dimensionality estimation.

2.3.1. LiDAR and Multi-spectral Data Fusion for Improved Tree Crown Segmentation

Detection of trees has been intensively studied previously, particularly within the application of remote sensing of forest environments. Whilst similar in concept, the environment in power line

corridor is more complex because the background is cluttered with shadows, bare soil, shrubs and grass, all presenting irregularities that need to be handled by the detection algorithm. Vegetation has a distinctive spectral signature, characterized by a low reflectance in the visible part of the solar spectrum, and a high reflectance in the near-infrared (NIR) region. Therefore, NIR information is widely used in the remote sensing community for the detection and classification of vegetation. Combining LiDAR elevation data can further improve tree detection by removing low-growing grass and shrubs. For classification of tree species, object-based methods are preferred as they are straightforward and have been shown to obtain higher classification accuracy in high resolution image classification (Blaschke 2010). To conduct an object-based classification, accurate individual tree segmentation is required. Subsequent to this, a range of classification algorithms can be used in the object-feature space.

As discussed in section 2.1.2, 2D image based tree crown segmentation algorithms often meet difficulties in discriminating grass, shrub and trees since these types of vegetation are often very similar in both color and texture. The 3D nature of LiDAR data makes it especially well suited to this situation. However, the success and quality of the results depend on the point density of LiDAR data as well as the size, shape and distribution of trees. Multi-spectral imagery provides spectral and texture information that is complementary to LiDAR information. Therefore, combining LiDAR data and multi-spectral imagery seems to be a promising way to improve individual tree crown detection and delineation. In this study, a region level fusion method is developed to combine multi-spectral image and LiDAR data for individual tree crown detection and delineation.

The first step towards fusing LiDAR and multi-spectral imagery is referencing. This step is also known as sensor alignment or registration and establishes a common reference frame for different sensor data. If the two sensors are mounted on the same aerial platform then the navigation system (GPS/IMU) provides position and attitude data for both the aerial camera and the LiDAR system. Since the GPS/IMU unit and the two sensors are physically separated, the success of sensor alignment relies on how well the relative position and attitude of the various system components can be determined. The multi-spectral imagery and LiDAR data used in our experiments have already been georeferenced by the commercial data provider, which simplifies the sensor fusion process.

Assuming that sensor alignment has been completed with sufficient accuracy, LiDAR data can then

be considered as an additional image layer of the multi-spectral imagery. After ground filtering, object points are obtained to refine the tree crown segmentation. The fusion process is described in Figure 5. First, LiDAR point cloud data and georeferenced multi-spectral imagery are processed separately. On one side, an initial segmentation is conducted in spectral feature space using the algorithm developed in (Li, Hayward, Zhang et al. 2009). After that, regions in the initial vegetation segmentation map are labeled for the following fusion process. On the other side, a ground filtering algorithm using statistical analysis is conducted to separate terrain and object points (Liu, Li, Hayward et al. 2009). Then the point clouds are converted to a 2.5D height image. The pixel size of the height image used in this paper is 15 centimeters, which is the same with multi-spectral image pixel. The lowest Z coordinate (height) within the bounds of a pixel is chosen as the height of that pixel. The 2.5D depth image is then integrated with the labeled vegetation segmentation map. A simple thresholding process is used in order to remove grass and low vegetation. The region mean height histogram is calculated to visualize the height difference among regions. The mean height of a region which contains grass and low vegetation points will be much lower than a region which contains only trees. Finally, a watershed-based segmentation (Bleau and Leon 2000) is employed to further decompose the tree clusters to individual trees.

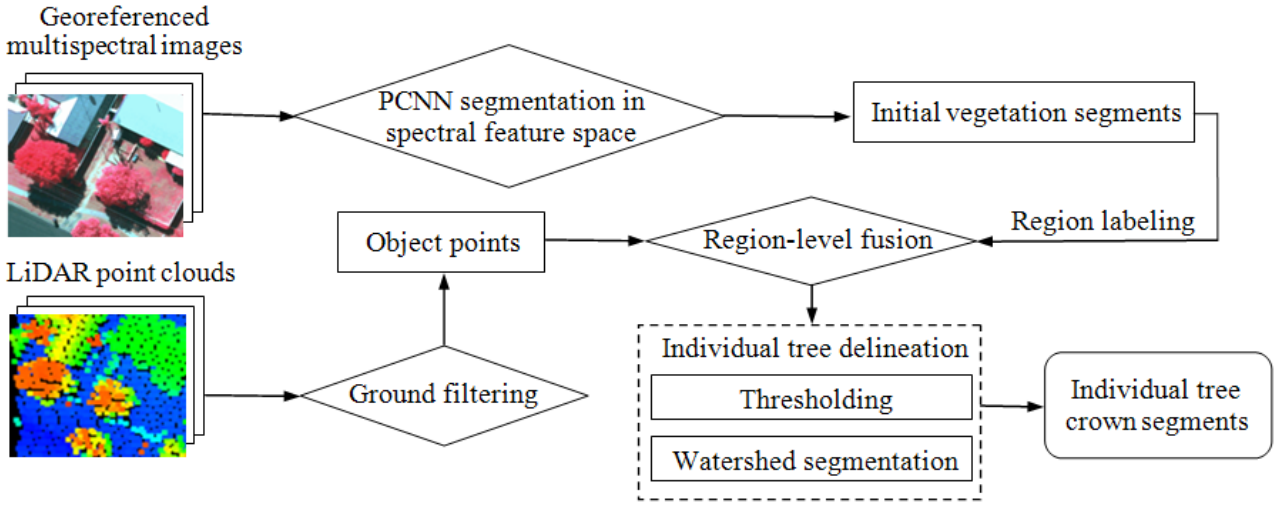

Figure 5 Framework of LiDAR and georeferenced multi-spectral imagery fusion for individual tree crown segmentation

2.3.2. Color and Texture Feature Fusion for Improved Tree Species Classification

After individual trees have been segmented, a number of local feature descriptors can be used to represent each tree crown. The use of appropriate features to characterize an output class or object is

fundamental for any classification problem. There is no generically best feature for image classification. The selection of an appropriate feature descriptor must reflect a specific classification task in hand and usually needs to be obtained through experimental evaluation. We have conducted a feature evaluation (Li, Hayward, Zhang et al. 2010) and developed a new rotation and scale invariant spectral-texture feature descriptor (Li, Hayward, Walker et al. 2011). The experimental results published in our previous work demonstrated that tree species classification performance can be considerably improved through careful design of feature descriptors. In this paper, we further evaluate the fusion of multiple color and texture features based on a kernel PCA based method.

Color and texture are two fundamental features in describing an image, but prior research has generally focused on extracting color and texture feature as separate entities rather than a unified image descriptor (Whelan and Ghita 2009). The idea of using both color and texture information has strong links with human perception, and these links motivates an investigation of how to effectively fuse color and texture as a unified descriptor to improve the discrimination over viewing color and texture features independently. Although the motivation of using color and texture information jointly in object-based image classification is clear, how best to combine color and texture in a unified object descriptor is still an open issue. Huang el al. (Huang, Zhang and Li 2008) proposed a multiscale spectral and spatial feature fusion method based on wavelet transform and evaluated in very high resolution satellite image classification. Zhang et al. (Zhang et al., 2008) extracted texture features using multi-channel Gabor filters and Markov random fields integrated the two features using a neighbourhood oscillating tabu search approach for high-resolution image classification (Zhang, Zhao, Huang et al. 2008). However, these methods extract features from fixed window size and do not consider all pixels within an object as a whole. Moreover, heavy computational burden is induced by combining multiple features (through 'the curse of dimensionality') and these burdens may limit the practical performance of the classifier.

It is often difficult to classify objects using a single feature descriptor. Therefore, feature-level fusion plays an important role when multiple features are used in the process of object classification. The advantages of feature fusion are: 1) the most discriminatory information from original multiple feature sets can be derived by the fusion process; 2) the noisy information can be eliminated from the correlation between different feature sets. In other words, feature fusion is capable of deriving and gaining the most effective and least-dimensional feature vectors that benefit the final classification (Yang, Yang, Zhang et al. 2003). The feature fusion framework is illustrated in Figure

6. After object segmentation, color and texture features are extracted from image objects. Different feature vectors are normalized and then serially integrated. After that, kernel PCA is used to globally extract the nonlinear features from the integrated feature sets as well as to reduce the dimensionality. The intrinsic dimensionality of the serial fused features is estimated using a maximum likelihood method to select the target dimensionality from the kernel PCA fused feature. Finally, features selected from Kernel PCA are used as the input to classifiers for further analysis.

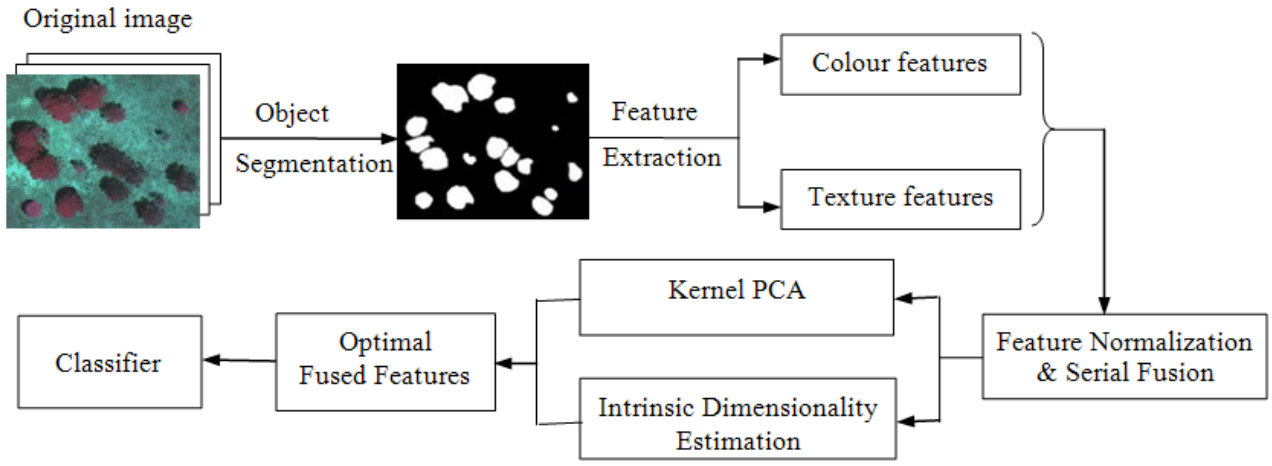

Figure 6 Framework of object-level color and texture feature fusion

We first use a serial fusion strategy by simply combining different feature vectors into one set of feature union-vector. Different features vectors are combined into one set of feature union-vector. As the features are different on the value scope, they are initialized into range [-1,1] by Gaussian criterion. Consider a n-dimensional feature vector $\boldsymbol{F} = \boldsymbol{f}_{ij}$, where $\boldsymbol{f}_{ij}$ is the $\boldsymbol{j}^{th}$ feature component in $\boldsymbol{F}_i$. Assuming that $\boldsymbol{f}_{ij}$ is a Gaussian sequence, we compute the mean $\boldsymbol{m}_j$ and the standard deviation δ_j. Feature $\boldsymbol{f}_{ij}$ is normalized by $\boldsymbol{f}'_{ij} = (\boldsymbol{f}_{ij} - \boldsymbol{m}_j)/\delta_j$. Suppose α and β are two feature vectors which are extracted from the same image-object. The integrated feature union-vector is defined by $\gamma = \begin{pmatrix} \alpha \\ \beta \end{pmatrix}$. Obviously, if feature vector α is m-dimensional and β is n-dimensional, then the dimension of feature vector γ is $\boldsymbol{m} + \boldsymbol{n}$.

Traditional linear feature selection and extraction methods such as PCA are conducted in the original input space, and thus cannot properly handle nonlinear relationships in the data (Cao, Shen, Sun et al. 2007). For example, the principal components of features may not be linearly related to the input variables and the features of different categories may not be simply separated by a

hyperplane. To solve this problem, kernel methods can be introduced to map original data to a kernel space using a mapping function. Kernel PCA is one of these kernel methods which reformulate traditional linear PCA in a high-dimensional space using a kernel function. Given $\boldsymbol{M}$ input vectors $\boldsymbol{x}_p$, kernel PCA firstly map the original input vectors $\boldsymbol{x}_p$ into a high-dimensional feature space $\phi(\boldsymbol{x}_p)$. Performing PCA in the high-dimensional feature space can obtain high-order statistics of the input variables, which is also the initial motivation of kernel PCA (Xie and Lam 2006). In PCA, the principal component of $\boldsymbol{x}_p$ is the product of $\boldsymbol{x}_p$ and the eigenvectors of the covariance matrix of $\boldsymbol{M}$ input vectors. However, it is difficult to directly compute both the covariance matrix of the high-dimensional feature space $\phi(\boldsymbol{x}_p)$ and its corresponding eigenvectors and eigenvalues in the high-dimensional feature space. Therefore, kernel tricks are employed to avoid this difficulty and the principal eigenvectors are computed from the kernel matrix, rather than the covariance matrix. More details of kernel PCA are introduced in the appendix of this paper.

Using kernel PCA to find the underlying structure of and the correlations of multiple feature sets has important benefits. First, the most discriminatory information can be derived and redundant information can be eliminated from the fusion process. Second, the dimension of feature sets can be reduced and thus the computational cost of the subsequent classification stage is reduced. However, it can still be difficult to find a suitable criterion for selecting optimal features using kernel PCA.

Up to this point we have assumed that the target dimensionality of the low-dimensional feature representation was known and specified by the user. In practice, the optimal dimensionality needs to be estimated automatically. A possible solution is to estimate the intrinsic dimensionality of the high-dimensional feature set and then use this estimate as the target dimensionality. Intrinsic dimensionality is the minimum number of variables that is necessary in order to represent all the information in a dataset. In this paper a maximum likelihood estimator (MLE) (Levina and Bickel 2004) is employed to estimate the intrinsic dimensionality. MLE is a local intrinsic dimensionality estimator which is based on the observation that the intrinsic dimensionality of the data manifold around one data point can be estimated by measuring the number of data points covered by a hypersphere with a growing radius. MLE considers the data points in the hypersphere as a Poisson process, in which the estimated intrinsic dimensionality d around data point x_i in given k nearest neighbours is given by

$$\hat{d}_k(x_i) = \left(\frac{1}{k-1} \sum_{j=1}^{k-1} \log \frac{T_k(x_i)}{T_j(x_i)} \right)^{-1} \quad (1)$$

where $T_k(x_i)$ represents the radius of the smallest hypersphere with centre x_i that covers k neighbouring data points.

Different numbers of neighbouring data points can be treated as the different scales. It was clear from equation (1) that the calculation of intrinsic dimension $\hat{d}$ depends on scale parameter k. In this paper, the intrinsic dimension is obtained by averaging $\hat{d}$ over a scale range $[k_1, k_2]$ using the following equations:

$$\hat{d}_k = \frac{1}{M} \sum_{i=1}^{M} \hat{d}_k(x_i) \quad (2)$$

$$\hat{d} = \frac{\sum_{j=k_1}^{k2} \hat{d}_k}{k_2 - k_1 + 1} \quad (3)$$

where $\hat{d}$ is the number of input vectors, $\hat{d}_k$ is the estimated dimension at scale k, and $\hat{d}$ is the final estimated dimensionality.

3. AIRBORNE PLATFORM CONTROL EXPERIMENTS AND RESULTS

3.1. Study of Swath Width Variation under Autopilot Control

Simulated and experimental flight test results of new guidance and control techniques for inspection of linear infrastructure that demonstrated improved cross-track and heading error performance in line tracking were previously published in (Bruggemann, Ford and Walker 2010). Here we present further results which illustrate the effect of aircraft position and orientation on swath coverage and corridor tracking performance under autopilot control. An experimental flight test was made of a Cessna 172 fitted with PTAGS tracking a 10 km section of powerline corridor at Kingaroy, Queensland, Australia. PTAGS commanded the aircraft autopilot for lateral control whilst the pilot maintained vertical control with average speed of 46 m/s and average altitude of 457 m above ground level. Aircraft position and orientation were recorded via a survey grade dual frequency GPS-INS system for later evaluation of the flight performance. Wind conditions included a 15 knot

south westerly wind and low turbulence. The next two sub-sections study the impact of terrain, altitude and aircraft bank angle on LiDAR swath width.

3.1.1. Impact of Terrain Variation on Swath Width

In this section, the impact of terrain variation on swath width is studied on the basis of aircraft flight data, including measured aircraft position and attitude, collected during a powerline inspection flight. A LiDAR sensor was not installed during this flight, but a fictitious LiDAR swath width (corresponding to a LiDAR swath pattern covering a 45 degree field of view) can be calculated from simple geometry. The situation is illustrated by Figure 7 and Figure 8 showing that the swath width for a lower altitude above ground (AGL) is smaller than the swath width for higher AGL (under level terrain assumption).

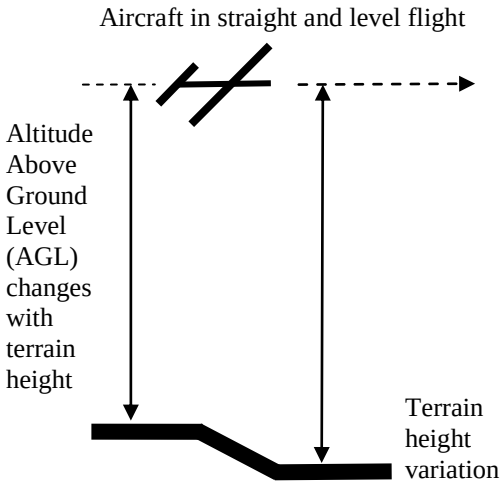

Figure 7 Changes in terrain height cause changes in altitude above ground (AGL), which will impact swath width.

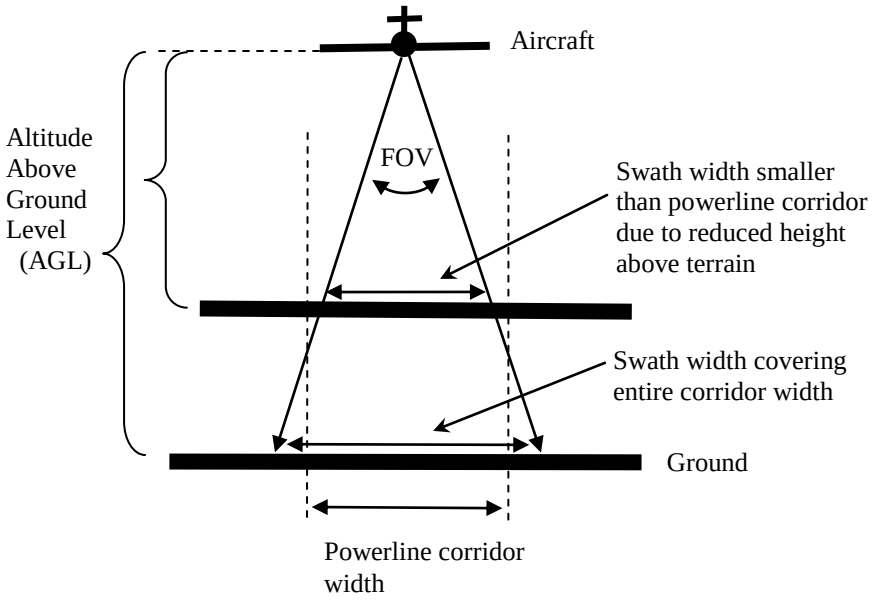

Figure 8 The effect of altitude above ground level (AGL) on swath width. The swath width for a lower AGL is smaller than the swath width for a higher AGL.

To isolate the impact of the terrain variations, the measured aircraft altitude will be ignored in the following swath calculations and only aircraft attitude and position information will be used (a mean altitude above ground of 457 m or 1500 ft will be assumed). A digital terrain elevation model was obtained for the flight test area and then a fictitious steady-rate climb flight profile was calculated that corresponds to a mean altitude of 457 m (1500 ft) above the terrain model, as shown in Figure 9. This fictitious vertical profile was assumed so that variations in estimated swath would be due only to terrain variation and roll motion (and not due to features of the experiment aircraft's altitude dynamics). Note that in practice there would be some vertical error in tracking the vertical flight profile under autopilot or manual pilot control which will introduce additional variation in swath width.

Using simple trigonometry, the swath width was then estimated on the basis of the terrain profile model, the assumed vertical flight profile, the measured aircraft position and attitude, and the width estimates for two different vertical flight profiles is shown in Figure 10. Because vertical effects have been removed, the variability of the estimated swath width is purely due to aircraft roll motion recorded from the flight test. For comparison purposes, the estimated swath width variation under the alternative assumption of a flat terrain profile (that is, constant altitude flight above a flat

terrain) is also shown in Figure 10. During the flight experiment there was an average 26 m and maximum 86 m swath width difference between considering the terrain variations and assuming flat terrain. The noticeable greater variability in swath width in the presence of terrain variation suggests that terrain variation impacts the swath width more significantly than aircraft roll motion. This highlights inspection challenges in terms of not only lateral but also vertical automatic control of the aircraft, and these challenges will impact LiDAR sensor considerations. However, this does not mean that roll motion should be disregarded, as will be seen in the next section.

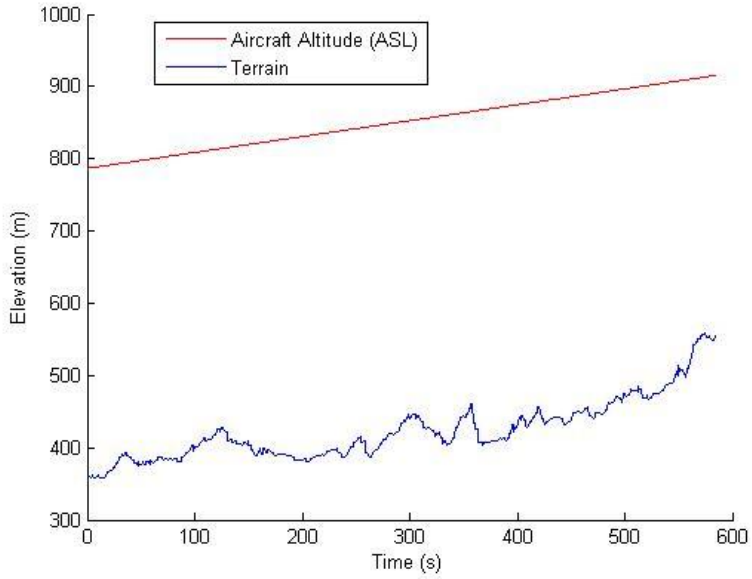

Figure 9 Aircraft steady climb (calculated), required to achieve a mean altitude of 457 m (1500 ft) above terrain.

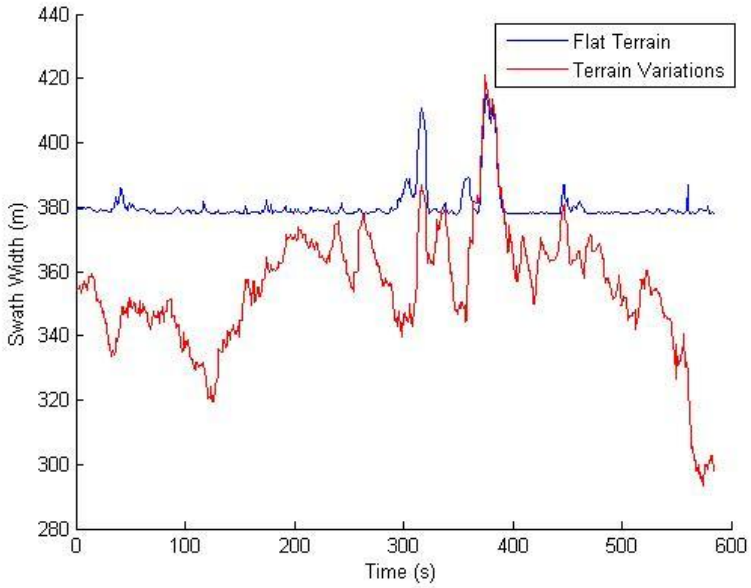

Figure 10 Impact of terrain variation on swath width showing a difference of up to 86 metres (at around 580 seconds) as compared to flat terrain.

3.1.2. Impact of Aircraft Bank Angle on Swath Width

Results examining swath width variation due to bank angle are now presented (whilst tracking a 15 km long section of powerline corridor using an aircraft under autopilot control). As illustrated by Figure 11, a non-zero bank angle can change the geometry causing the swath width to change, but more significantly a non-zero bank angle might cause the swath width to not cover the entire corridor width.

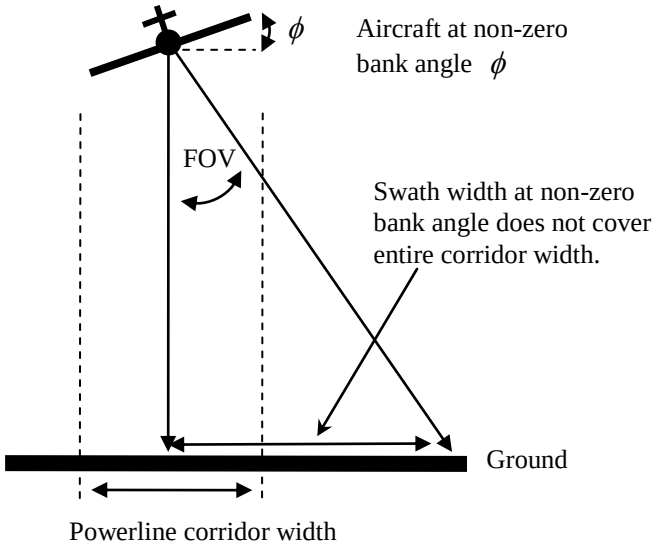

Figure 11 Impact of Aircraft Bank Angle on Swath Width (with flat ground assumption).

Figure 12 shows the swath variation (estimated swath including terrain variation, as explained in previous section) due to bank angle for a Cessna 172 tracking powerlines under autopilot control using the precision guidance and control algorithms presented in (Bruggemann, Ford and Walker 2010). A desirable corridor width of 200 m was assumed and is displayed on the figure as the red lines.

The PTAGS successfully maintained swath coverage over 98% of the corridor region. However there was one part of the corridor missed due to excessive roll angle, as indicated by A on the figure. Note that during the flight experiment the aircraft roll angle did not exceed 15 degrees (due to the rate-1 turn limitation of the autopilot).

From these results it is evident that the aircraft bank (which is necessary to change the heading of the aircraft and maintain lateral track over the corridor) has the undesirable but unavoidable effect of moving the swath region away from the corridor to be inspected. Thus, autopilot guidance and control algorithms for aerial inspection must make tradeoffs between accurate position track over the corridor and constraining the roll so that the complete corridor region is measured. Both desired roll changes (to effect a heading change) and undesired roll changes (such as due to wind gusts) present a challenge for automatic control of the airborne platform for tracking powerline corridors. This problem is magnified in smaller aircraft or UAVs that are more susceptible to wind gusts. Although roll stabilized sensor systems exist, stabilization of the sensor head does not solve all issues associated with excessive roll angle. For example, excessive aircraft roll might cause loss of lock of GPS satellites (GPS is typically integrated in LiDAR survey systems to provide the aircraft's absolute position). Also, the amount of roll stabilization offered by commercially available LiDAR aerial survey systems is often limited to small angles due to the additional expense in terms of captured data quantity or quality. It is therefore desirable to mitigate unwanted roll motion via design of better control of the aircraft platform. Better aircraft roll behavior might be achieved via maneuver selection strategies, and the use of constrained bank or skid turns as proposed in (Bruggemann, Ford and Walker 2010; Mills, Ford and Mejias 2011) .

A feature of the specialized powerline tracking and guidance algorithms is that the aircraft ground track cuts across the powerline corners (observe the behavior of the blue line of Figure 12). A small

corner of corridor that was missed due to track error (introduced by the "cutting across the corner" feature of the guidance algorithm) is indicated on Figure 12 by B. This highlights an issue in tracking short line segments with sharp changes in line direction – a decision is required on whether or not to proceed to "cut across the corner" or command a complete turn such that the complete segment is captured. This is essentially a tradeoff between flight efficiency and certainty of data capture. That is, a complete turn could be conducted at every change in corridor direction to help ensure corners are not missed, but this would be inefficient in terms of flying time and distance. On the other hand, a "cutting across corner" approach at every change in corridor direction may result in missing parts of the corridor as seen on the figure. This decision could be made in-flight based upon the known angular change in corridor direction with a predictive swath coverage model, or made in pre-flight planning. The automatic turn performance of PTAGS in conducting complete turns around corners will be presented in the following section.

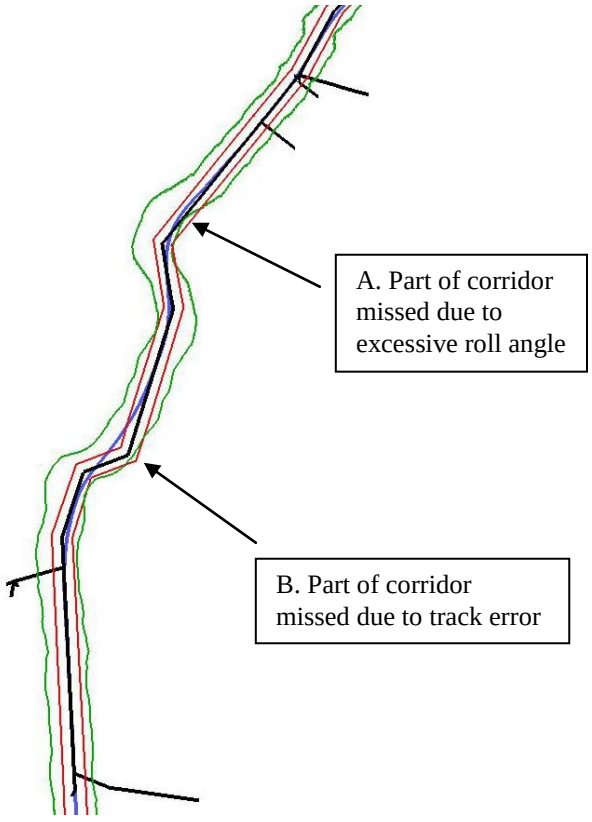

Figure 12 Tracking a 15 km long powerline corridor under autopilot control with PTAGS. Black – powerline corridor centre, red – 200 m wide powerline corridor, green - swath width (accounting for terrain variation and aircraft bank angle), blue – aircraft ground track. The results demonstrate

successful coverage of the corridor under autopilot control for most of the corridor, with occasional miss of corridor (as indicated by A and B on figure).

3.2. Demonstration of Automatic Turn Capability around Corridor Corners

When tracking powerline corridors, a key requirement is that when the aircraft turns around between two line segments the aircraft can successfully maintain lateral stability whilst returning on track towards the next line segment without missing the corner of corridor where the two segments meet. This section presents results that illustrate the automatic turn capability of PTAGS around corners. A test case consisting of three line segments connected by 90 degree changes in direction was constructed as shown by the black lines on Figure 10. These line segments were flown by the Cessna under autopilot control using PTAGS which automatically calculated and flew turns between each segment. If PTAGS detected that it could not get back on track to the next line segment without missing the corridor PTAGS automatically triggered a "go-around again" maneuver.

On Figure 10 the ground-track of the aircraft is shown by the red lines (the trajectories shown correspond to the power lines being inspected twice). The aircraft successfully executed 90 degree cornering maneuvers without the sensor swath width missing the corners. During one of the cornering maneuvers the aircraft missed the start of the powerline corridor at the top corner due to wind gusts. However the PTAGS automatically triggered a "go-around again" maneuver to ensure inspection is complete (hence the three turns shown at the top corner compared to two turns shown at the bottom corner). This automated "go-around again" maneuver demonstrates the dynamic re-planning capability of the system under autopilot control. Finally, some lateral instability can be seen on straight segments which may indicate some algorithm tuning or refinement is required.

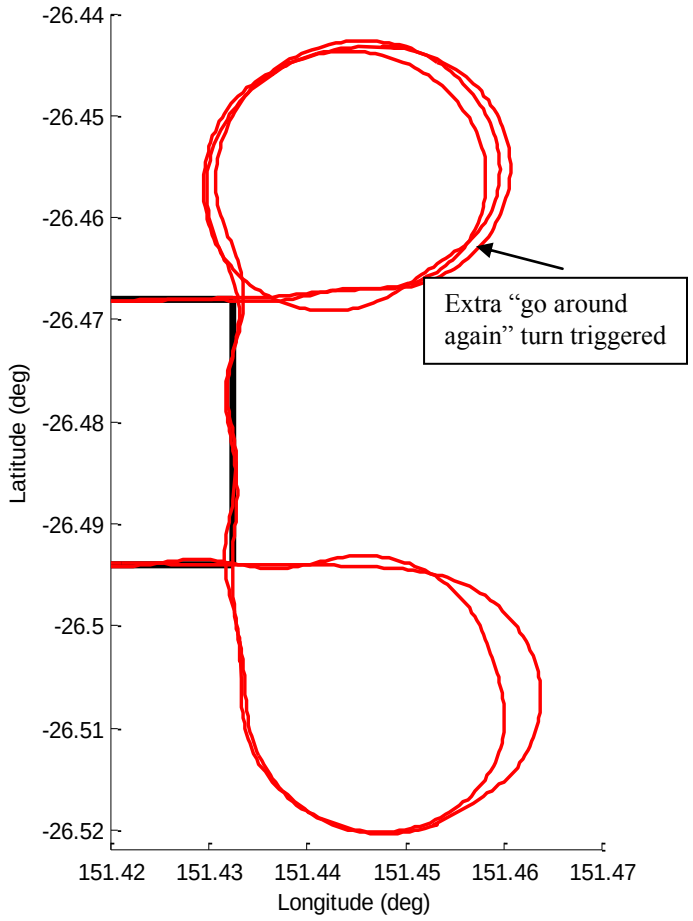

Figure 13 Automatic turning around 90 degree corners with PTAGS, demonstrating successful tracking of lines after turns and triggering of a "go-around again" maneuver. Black lines – line segments. Red lines – aircraft ground track.

4. AUTOMATED DATA PROCESSING EXPERIMENTS AND RESULTS

4.1. Data Collection

In this study, both aerial remote measurements and ground survey data were collected. The first series of flights (conducted by a local company) collected data from a high resolution digital 4-band multi-spectral camera (DuncanTech MS-4100) with a DGPS/INS mounted in the cargo area of a Piper Cub. In these flights, multi-spectral data was captured over 4 spectral bands: NIR (800-966nm), red (670-840nm), green (540-640nm), blue (460-545nm) whilst traveling at approximately 34m/s (65 knots) at an altitude of 350m AGL(multi-spectral images were captured at approximately 15cm GSD). The second series of flights (conducted by a different local company) collected data

from an airborne LiDAR scanner mounted onto a Cessna aircraft. In these flights, the LiDAR data was collected with a scan angle of $\pm 30°$ with an average sample rate of 9 points per square meter. Figure 14 shows the data collection systems.

(a) Multi-spectral imagery collection system

(b) Lidar data collection system

Figure 14 Data Collection Systems

The ground survey was conducted in a 1.5 kilometer corridor in the towns of Murgon and Wondai in Central East Australia where the above identified multi-spectral image and LiDAR data were collected. The ground truth data of vegetation species were obtained with domain experts' participation. Figure 15 shows a mosaic of the test area generated from aerial images acquired from the trial. It should be noted that classifying all types of species in power line corridors requires significantly more resources than are currently available; however, classifying species in a given test area as a proof of concept is possible. In this research, we focus on three dominant species in our test field: Eucalyptus tereticornis, Eucalyptus melanophloia, and Corymbia tesselaris. We abbreviate the species names to Euc-Ter, Euc-Mel and Cor-Tes.

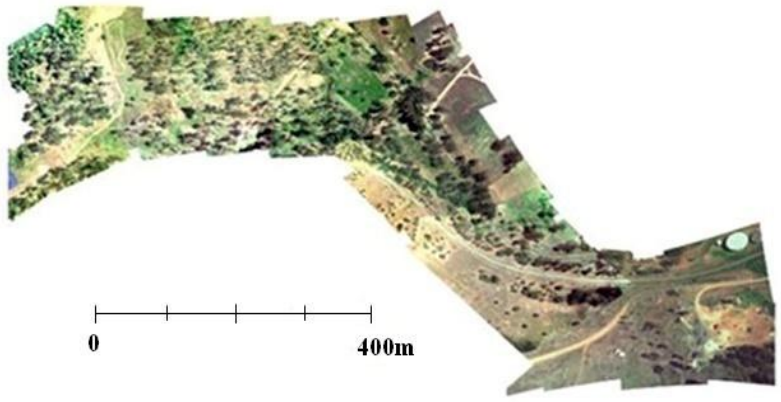

Figure 15 Experiment test site

4.2. LiDAR and Image Data Fusion

Figure 16 shows a pair of CIR image and LiDAR point cloud data in urban areas. Figure 17 shows the fusion process and the result using the image and LiDAR data. As shown in Figure 17 (a), an initial segmentation was conducted on the CIR image without any post-processing. The initial segmentation detects trees as well as other vegetation segments (e.g. grass). Figure 17 (b) shows the 2.5D depth image of LiDAR object points after ground filtering. Each connected region in the initial segmentation map was labeled, showing different colors in Figure 17 (c). The 2.5D depth image is then integrated with the labeled vegetation segments map. A simple thresholding process is used in order to remove grass and low vegetation. An overlay of the LiDAR points after the fusion process on the initial segmentation map is shown in Figure 17 (d). From this figure, we can see that the low mean height regions representing grass and other low vegetation were separated. Figure 17 (e) shows the tree segments after the fusion process. Afterwards, a watershed algorithm was applied on the Figure 17 (e) to decompose the tree clusters to individual tree crowns. As can be seen from the final segmentation result, low vegetation regions have been successfully removed. However, a critical limitation from this fusion process is that it depends on the high point density of LiDAR data. For a small-sized tree crown and low point density LiDAR data, no points or only a few points hit the tree which may cause the tree to be removed due to low region mean height. A series of 13 pairs of multi-spectral imagery and LiDAR data were selected for processing with a total number of 183 trees. Frames were removed from the full sequence of images to minimize image overlap (overlap might see some trees processed more than once). Furthermore, the developed algorithm was only applied to those areas of the image that contained the power-line corridor. The developed

tree crown segmentation algorithm achieved a detection rate of 97.27% and a segmentation accuracy of 84.7%.

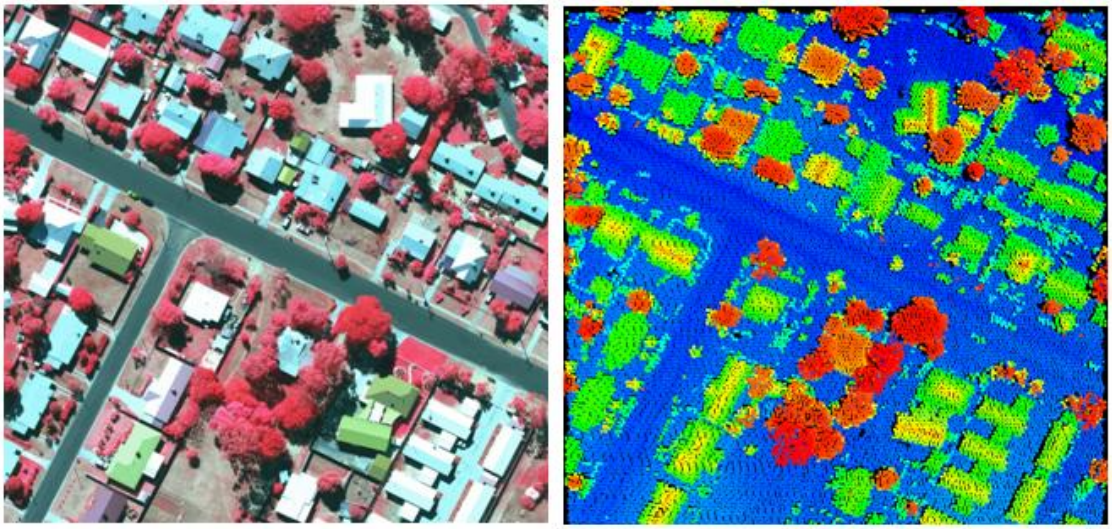

(a) CIR image (b) LiDAR point cloud data

Figure 16 A pair of the collected multi-spectral image and LiDAR point cloud data

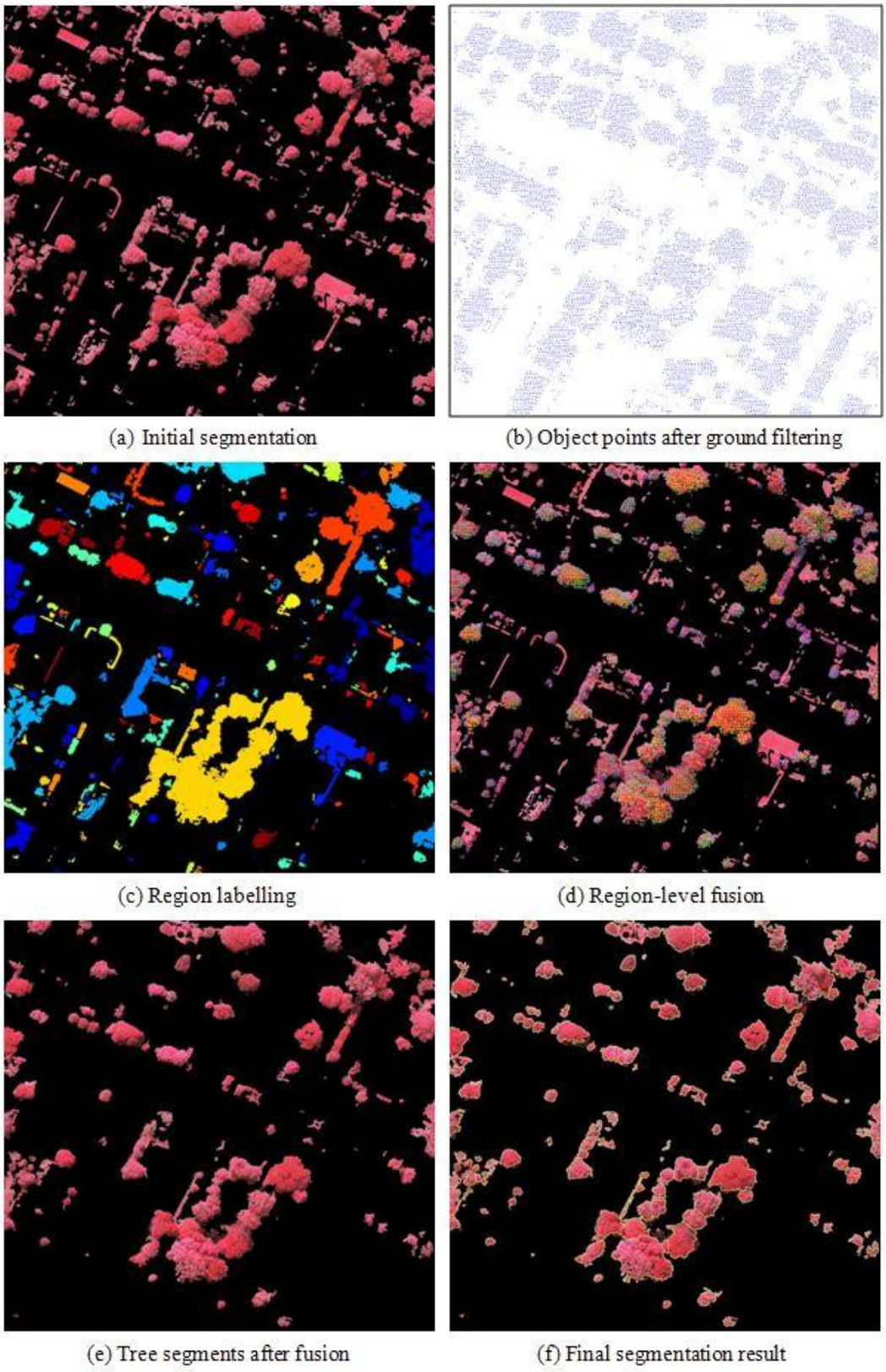

Figure 17 Fusion of LiDAR and multi-spectral imagery for individual tree crown segmentation

4.3. Color and Texture Feature Fusion

In order to select the most appropriate features for tree species classification, we have evaluated a number of state-of-the-art local feature descriptors and machine learning classifiers (Li, Hayward, Zhang et al. 2010; Li, Hayward, Walker et al. 2011). The evaluation results demonstrated that the classification success varies between different feature descriptors and classifiers. Overall, the rotational and scale invariant spectral-texture feature developed in (Li, Hayward, Walker et al. 2011) showed the best overall classification accuracy and support vector machine (SVM) was suggested as it generally obtains robust classification performance. In this paper, we extend the same strategy to evaluate the performance of the feature fusion method with a SVM classifier. The V-fold cross validation technique was employed in the experiment, and 10 folders were selected for the cross validation. The dataset is partitioned into 10 groups, which is done using stratification methods so that the distributions of categories of the target variable are approximately the same in the partitioned groups. Then 9 of the 10 partitions are collected into a pseudo-learning dataset and a classification model is built using this pseudo-learning dataset. The rest 10% (1 out of 10 partitions) of the data that was held back and used for testing the built model and the classification error for that data is computed. After that, a different set of 9 partitions is collected for training and the rest 10% is used for testing. This process is repeated 10 times, so that every row has been used for both training and testing. The classification accuracies of the 10 testing datasets are averaged to obtain the overall classification accuracy.

Two classic color and texture features, color histogram and local binary pattern (LBP) (Ojala, Pietikainen and Maenpaa 2002) are tested in the experiment. The overall classification accuracies of the fused color-texture feature were compared with single color and texture feature vectors and serial integrated feature vector through the same classifier. For comparison purpose, another widely used nonlinear feature selection technique, Generalized Discriminant Analysis (GDA), is also evaluated in the experiment. GDA is also known as Kernel Linear Discriminant Analysis (Kernel LDA), it is the reformulation of LDA in the high dimensional space constructed using a kernel function (Baudat and Anouar 2000). In this experiment, a Gaussian kernel function is used to construct GDA for the fusion of color-texture features.

From the experiment, the overall classification accuracies of color histogram and LBP texture features are 76.03% and 71.07% respectively. The serial integration of these two features shows

better performance over single feature with an overall accuracy of 83.47%. To evaluate of performance of fused feature using kernel PCA, we use a step-by-step model justification method (Song and Tao 2010). We justify the dimensionality from 2 to 8 with steps of 2, and from 10 to 100 with steps of 10, for the fused feature vectors. Figure 18 shows the classification accuracy curve at different dimensions. As we can see from the figure, the kernel PCA fused feature performs much better than single feature and serial integrated feature. However, the kernel PCA fused feature is still based on the assumption that user can specify a good target dimensionality. The estimation of intrinsic dimensionality using MLE is employed as the automatic selection of optimal number of dimensions. From our experiment, the intrinsic dimensionality of the integrated LBP and Color histogram feature is 39.3016, which conforms to the result from Figure 18 where the best accuracy (95.04%) is obtained at dimension 40.

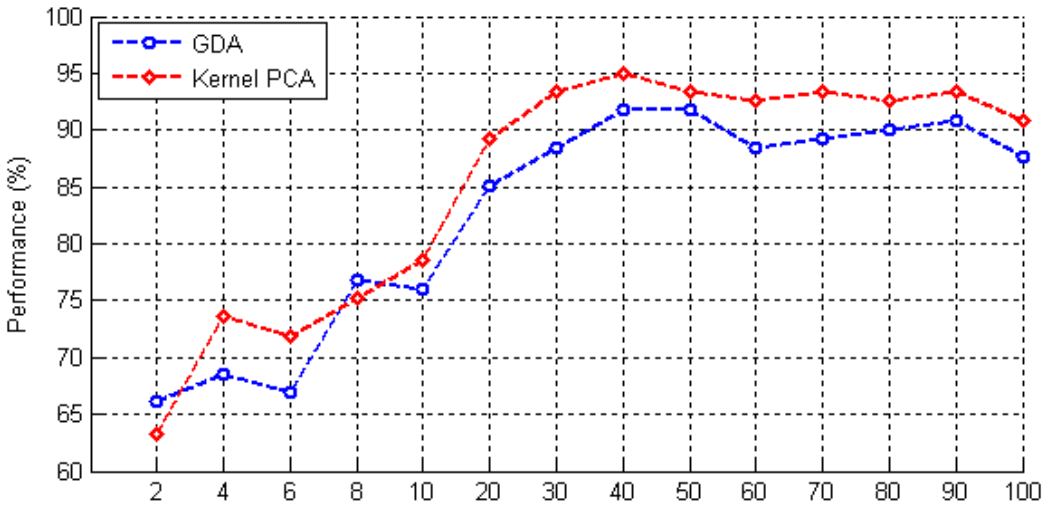

Figure 18 Classification accuracies of the fused features at different dimensions

Table 1 The classification results of single and fused color and texture features

	Hist_RGBNIR	LBP	Serial Fusion	KPCA-40	GDA-40
Overall Accuracy	76.03%	71.07%	83.47%	95.04%	91.73%
Analysis Time	79.46 s	246.29 s	305.83 s	13.63 s	4.63 s

In the experiment, the computational costs of the classifiers using different feature vectors are also compared. The analysis time is recorded under a desktop PC configuration of core duo 2.66GHz CUP and 2GB memory. Table 1 summarizes the overall accuracies and analysis time using different feature sets. The optimal dimension of kernel PCA and GDA fused feature is 40, which is derived from the estimation of the intrinsic dimensionality. From the results, we can see that the analysis

time varies a lot for different feature sets. High dimensionality of the original color and texture features and the serial fused feature cause high computational costs, while the using the nonlinear fusion method like kernel PCA and GDA can not only improve the classification accuracy but also significantly reduce the dimensionality and the computational costs.

From the experimental results, it is clear that fusion of color and texture features provides improved discriminative power over using them independently. Moreover, the proposed nonlinear feature fusion strategy using kernel PCA has shown great improvement over the serial fusion strategy, not only on reducing the dimensionality and computational cost, but also on removing noisy information and improving the discriminative power. The proposed feature fusion strategy can be extended to combine any other feature vectors if they are considered to have some complementary information.

(a) tree crown detection and segmentation

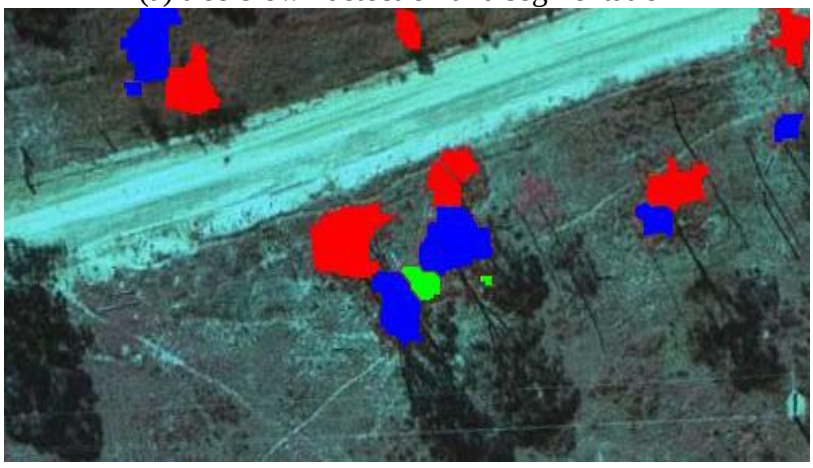

(b) classification map (species are represented using different colors)

Figure 19An example of Individual Tree Segmentation and Species Classification

Figure 19 shows an example of individual tree crown segmentation and classification map. It should be noted that trees can often appear differently in different seasons and even the same tree species may vary due to their health status. The data that was available did not provide the opportunity to classify the same vegetation under different conditions. Therefore, more variables may need to be considered to model a specific tree species more accurately in future work.

5. CONCLUSION AND FUTURE WORK

This paper comprehensively investigated the use of aerial remote sensing techniques for power line corridor monitoring and vegetation management. A technology overview and a series of experiments and results are presented. The major technological contributions and the lessons we learnt are summarized as follows:

- **Automatic Control of Airborne Platform**

Currently, standard industry practice is to fly powerline corridors under manual piloted control. This mode of flying over extensive powerline infrastructure on a routine basis is seen to be dangerous and tedious, justifying the development of autopilot technologies which may assist a human pilot and eventually lead to complete autonomous UAV solutions for more efficient and safer operations.

The Powerline Tracking Automatic Guidance System (PTAGS) developed at ARCAA specifically for tracking powerline corridors attempts to address some of the horizontal control problems and showed satisfactory performance in tracking powerline corridors. Experimental results demonstrated the impact of roll angle and terrain variation on swath width which must be considered for an aircraft under autopilot control tracking powerline corridors. The key challenges lie in the lateral and vertical automatic control of the aircraft as both consideration of translational and rotational motion is required. Further work is required to address these challenges further and extend the approach to also consider vertical motion.

- **Reliable and Automated Data Processing**

The information derived from multi-sensor data and various modeling approaches provides the opportunity to increase the reliability of the information extraction for robust operational performance and decision making in corridor monitoring (e.g. improved classification, increased confidence and reduced ambiguity). By fusing LiDAR with multi-spectral imagery and also color with texture features, we were able to significantly improve tree segmentation and species

classification. The next stage is to apply the same fusion strategy to combine geometric features derived from LiDAR data and the spectral-texture features derived from multi-spectral imagery. Effective fusion of multi-sensor, multi-resolution, multi-temporal and multi-platform image data, together with geospatial data and GIS represents the future solution for smart power line corridor monitoring.

The presented methods for object recognition (i.e. power lines and trees) are designed for off-line use. Data is collected, stored in a repository and analyzed at some later time. Real-time processing of data would be beneficial if useful information could be extracted that assists in the decisions made by the aircraft control system. For example, real-time power line detection can be used for the purposes of active aircraft guidance in situations where there is no or limited prior knowledge about the network (e.g. GPS locations of power line are not accurately known). Alternatively, the real-time identification of regions outside the immediate vicinity of the power-line where vegetation is sparse could be used to reduce the resolution of data stored. Questions concerning the algorithms and computing architectures that are best suited to increase the autonomy of a UAV capturing significant amounts of data need to be addressed in future work.

APPENDIX

Kernel Principal Component Analysis (PCA)

Assuming that the kernel matrix is centered, i.e. $\sum_{p=1,q=1}^{M} K(x_p, x_q) = 0$, introducing the kernel matrix K makes the mapping implicit without manipulating high dimensional space $\phi(x_p)$ explicitly in terms of Mercer's condition. Each element of K is an inner product in the high-dimensional space (i.e. $K(x_p, x_q) = \phi(x_p) \cdot \phi(x_q)$). Assuming C is the covariance matrix of $\phi(x_p)$, μ_i and β_i are the i^{th} eigenvalue and eigenvector of C respectively, λ_i and α_i are the i^{th} eigenvalue and eigenvector of the kernel matrix the K. The relationships between eigenvectors and eigenvalues of C and K are

$$\mu_i = \frac{\lambda_i}{M} \tag{4}$$

$$\beta_i = \sum_{j=1}^{M} \alpha_i^j \times \phi(x_j) \tag{5}$$

where α_i^j is the j^{th} element of α_i $(j = 1, \cdots, M)$.

In order to obtain low dimensional feature representation, the data is projected onto the eigenvectors of the covariance matrix C. The result of low-dimensional data representation Y is obtained by computing the principal eigenvectors of components of x_p in the space $\phi(x_p)$.

$$y_p^i = \sum_{j=1}^{M} \tilde{\alpha}_i^j \times K(x_j, x_p) \tag{6}$$

where y_p^j is the i^{th} element of y_p and $\tilde{\alpha}_i$ is the normalized α_i $(\tilde{\alpha}_i = \alpha_i / \sqrt{\lambda_i})$.

The mapping performed by kernel PCA relies on the choice of the kernel function. In this paper, Gaussian kernel is employed which is widely used in many applications. The kernel function is defined as:

$$K(x_i, x_j) = exp\left(- \frac{\left\| x_i - x_j \right\|^2}{2\delta^2} \right) \tag{7}$$

Where δ is shape parameter.

ACKNOWLEDGEMENTS

This work was conducted within the CRC for Spatial Information, established and supported under the Australian Government's Cooperative Research Centers Programme, and sees collaboration between the Queensland University of Technology (QUT), the Australian Research Centre for Aerospace Automation (ARCAA) and Ergon Energy Australia. The authors gratefully acknowledge the contributions of Professor Rodney Walker, Dr Ross Hayward and Mr Ryan Fechney. The contributions of Bred Jeffers from Greening Australia and David Wood from Ergon Energy for their assistance in the field survey are also acknowledged.

REFERENCES

Baudat, G. and F. Anouar (2000). "Generalized discriminant analysis using a kernel approach." Neural Computation **12**(10): 2385-2404.

Beltrame, A. M. K., M. G. M. Jardini, R. M. acbsen and J. A. uintanilha (2007). Vegetation identification and classification in the domain limits of powerlines in Brazilian Amazon forest. IEEE International Geoscience and Remote Sensing Symposium**:** 2314-2317.

Berni, J. A. J., P. J. Zarco-Tejada, L. Suárez and E. Fereres (2009). "Thermal and narrowband multispectral remote sensing for vegetation monitoring from an unmanned aerial vehicle." IEEE Transactions on Geoscience and Remote Sensing **47**(3): 722-738.

Blaschke, T. (2010). "Object-based image analysis for remote sensing." ISPRS Journal of Photogrammetry & Remote Sensing **65**(1): 2-16.

Bleau, A. e. and L. J. Leon (2000). "Watershed-based segmentation and region merging." Computer Vision and Image Understanding **77**(3): 317-370.

Breidenbach, J., E. Næsset, V. Lien, T. Gobakken and S. Solberg (2010). "Prediction of species specific forest inventory attributes using a nonparametric semi-individual tree crown approach based on fused airborne laser scanning and multispectral data." Remote Sensing of Environment **114**: 911-924.

Bruggemann, T. S., J. J. Ford and R. A. Walker (2010). "Control of Aircraft for Inspection of Linear Infrastructure." IEEE Transactions on Control Systems Technology **PP**(99): 1-1.

Cao, B., D. Shen, J.-T. Sun, Q. Yang and Z. Chen (2007). Feature selection in kernel space. Proceedings of the 24th International Conference on Machine Learning, Corvallis, Oregon.

Chaput, L. J. (2008). Understanding LiDAR data - how utilities can get the maximum benefits from 3D modelling. International LiDAR Mapping Forum. Denver, USA.

Chitsaz, H. and S. LaValle (2007). Time-optimal paths for a dubins airplane. IEEE Conference on Decision and Control. New Orleans, USA.

Costa, B. M., T. A. Battista and S. J. Pittman (2009). "Comparative evaluation of airborne LiDAR and ship-based multibeam SoNAR bathymetry and intensity for mapping coral reef ecosystems." Remote Sensing of Environment **113**(5): 1082-1100.

Deng, Y. and B. S. Manjunath (2001). "Unsupervised segmentation of color-texture regions in images and video." IEEE Transactions on Pattern Analysis and Machine Intelligence **23**(8): 800-810.

Egbert, J. and R. W. Beard (2007). Low altitude road following constraints using strap-down EO cameras on miniature aerial vehicles. The American Control Conference, New York City, USA.

Erikson, M. (2003). "Segmentation of individual tree crowns in colour aerial photographs using region growing supported by fuzzy rules." Canadian Journal of Forest Research **33**(8): 1557-1563.

Erikson, M. and K. Olofsson (2005). "Comparison of three individual tree crown detection methods." Machine Vision and Applications **16**(4): 258-265.

Frew, E., T. McGee, Z. Kim, X. Xiao, S. Jackson, M. Morimoto, S. Rathinam, J. Padial and R. Sengupta (2004). Vision-based road-following using a small autonomous aircraft. IEEE Aerospace Conference.

Gurtner, A., D. G. Greer, R. R. Glassock, L. Mejias, R. Walker and W. W. Boles (2009). "Investigation of fish-eye lenses for small-UAV aerial photography." IEEE Transactions on Geoscience and Remote Sensing **47**(3): 709-721.

Holmgren, J., Å. Persson and U. Söderman (2008). "Species identification of individual trees by combining high resolution LiDAR data with multi-spectral images." International Journal of Remote Sensing **29**(5): 1537-1552.

Holt, R. S. and R. W. Beard (2010). "Vision-based road-following using proportional navigation." Journal of Intelligent and Robotic Systems **57**(1-4): 193-216.

Huang, X., L. Zhang and P. Li (2008). "A multiscale feature fusion approach for classification of very high resolution satellite imagery based on wavelet transform." International Journal of Remote Sensing **29**(20): 5923-5941.

Ituen, I. and G. Sohn (2010). "The way forward: advances in maintaining right-of-way of transmission lines." Geomatica **64**(4): 451-462.

Jones, D., I. Golightly, J. Roberts, K. Usher and G. Earp (2005). Power line inspection - a uav concept. The IEE Forum on Autonomous Systems. London, United Kingdom.

Jwa, Y., G. Sohn and H. B. Kim (2009). Automatic 3D power line resconstruction using airborne lidar data. ISPRS Laserscanning 2009. Paris, France.

Kobayashi, Y., G. G. Karady, G. T. Heydt and R. G. Olsen (2009). "The utilization of satellite images to identify trees endangering transimission lines." IEEE Transactions on Power Delivery **24**(3): 1703-1709.

Kwak, D.-A., W.-K. Lee, J.-H. Lee, G. S. Biging and P. Gong (2007). "Detection of individual trees and estimation of tree height using LiDAR data." Journal of Forest Research **12**(6): 425-434.

Leckie, D., F. Gougeon, D. Hill, R. Quinn, L. Armstrong and R. Shreenan (2003). "Combined high-density lidar and multispectral imagery for individual tree crown analysis." Canadian Journal of Remote Sensing **29**(5): 633-649.

Lefsky, M. A. and W. B. Cohen (2003). Selection of remotely sensed data. Remote Sensing of Forest Environments: Concepts and Case Studies. M. A. Wulder and S. E. Franklin. Dordrecht Kluwer Academic Publishers**:** 13-46.

Levina, E. and P. J. Bickel (2004). Maximum likelihood estimation of intrinsic dimension. Advances in Neural Information Processing Systems, The MIT Press. **17**.

Li, Z., R. Hayward, R. Walker and Y. Liu (2011). "A biologically inspired object spectral-texture descriptor and its application to vegetation classification in power line corridors." IEEE Geoscience and Remote Sensing Letters **8**(4): 631-635.

Li, Z., R. Hayward, J. Zhang, H. Jin and R. Walker (2010). "Evaluation of spectral and texture features for object-based vegetation species classification using support vector machines." International Archives of the Photogrammetry, Remote Sensing and Spatial Information Sciences **XXXVIII**(Part 7A).

Li, Z., R. Hayward, J. Zhang and Y. Liu (2008). Individual tree crown delineation techniques for vegetation management in power line corridor. Digital Image Computing: Techniques and Applications (DICTA), Canberra, IEEE Computer Society.

Li, Z., R. Hayward, J. Zhang, Y. Liu and R. Walker (2009). Towards automatic tree crown detection and delineation in spectral feature space using PCNN and morphological reconstruction. IEEE International Conference on Image Processing, Cairo, Egypt.

Li, Z., Y. Liu, R. Walker, R. Hayward and J. Zhang (2010). "Towards automatic power line detection for a UAV surveillance system using pulse coupled neural filter and an improved Hough transform." Machine Vision and Applications **21**: 677-686.

Liu, Y., Z. Li, R. Hayward, R. Walker and H. Jin (2009). Classification of airborne lidar intensity data using statistical analysis and Hough transform with application to power line corridors. International Conference on Digital Image Computing: Techniques and Applications. Melbourne, Australia, IEEE.

Lu, M. L. and Z. Kieloch (2008). "Accuracy of transmission line modeling based on aerial LiDAR survey " IEEE Transactions on Power Delivery **23**(3): 1655-1663.

Mallinis, G., N. Koutsias, M. Tsakiri-Strati and M. Karteris (2008). "Object-based classification using Quickbird imagery for delineating forest vegetation polygons in a Mediterranean test site." ISPRS Journal of Photogrammetry & Remote Sensing **63**: 237-250.

Mills, S., J. J. Ford and L. Mejias (2011). "Vision based control for fixed wing UAVs inspecting locally linear infrastructure using skid-to-turn maneuvers." Journal of Intelligent and Robotic Systems **61**(1): 29-42.

Mills, S. J., M. P. Gerardo, Z. Li, J. Cai, R. Hayward, L. Mejias and R. Walker (2010). "Evaluation of aerial remote sensing techniques for vegetation management in power line corridors." IEEE Transactions on Geoscience and Remote Sensing **48**(9): 3379-3390.

Nelson, D. R., D. B. Barber, T. W. McLain and R. W. Beard (2006). Vector field path following for small unmanned air vehicles. American Control Conference. Minneapolis, Minnesota, USA.

Nelson, D. R., D. B. Barber, T. W. McLain and R. W. Beard (2006). Vector field path following for small unmanned air vehicles. American Control Conference, Minneapolis, Minnesota, USA.

Niculescu, M. (2001). Lateral track control law for aerosonde UAV. The 39th AIAA Aerospace Sciences Meeting and Exhibit, Reno, NV.

Ojala, T., M. Pietikainen and T. Maenpaa (2002). "Multiresolution grey-scale and rotation invariant texture classification with local binary patterns." IEEE Transactions on Pattern Analysis and Machine Intelligence **24**(7): 971-987.

Pouliot, D. A., D. J. King, F. W. Bell and D. G. Pitt (2002). "Automated tree crown detection and delineation in high-resolution digital camera imagery of coniferous forest regeneration." Remote Sensing of Environment **82**(2-3): 322-334.

Pouliot, D. A., D. J. King and D. G. Pitt (2005). "Development and evaluation of an automated tree detection-delineation algorithm for monitoring regeneration coniferous forests." Canadian Journal of Forest Research **35**(10): 2332-2345.

Rathinam, S., Z. Kim, A. Soghikian and R. Sengupta (2005). Vision based following of locally linear structures using an unmanned aerial vehicle. The 44th IEEE Conference on Decision and Control, and the European Control Conference, Seville, Spain.

Rautiainen, M. (2005). The spectral signature of coniferous forests: the role of stand structure and leaf area index. Faculty of Agriculture and Forestry, Faculty of Agriculture and Forestry. Helsinki, University of Helsinki, Finland.

Ren, W. and R. W. Beard (2004). "Trajectory tracking for unmanned air vehicles with velocity and heading rate constraints." IEEE Transactions on Control Systems Technology **12**(5): 706-716.

Song, D. and D. Tao (2010). "Biologically inspired feature manifold for scene classification." IEEE Transactions on Image Processing **19**(1): 174-184.

Sugumaran, R., M. K. Pavuluri and D. Zerr (2003). "The use of high-resolution imagery for identification of urban climax forest species using traditional and rule-based classification approach." IEEE Transactions on Geoscience and Remote Sensing **41**(9): 1933 - 1939

Sun, C., R. Jones, H. T. X. Wu, K. Cheong, R. Beare, M. Buckley and M. Berman (2006). "Measuring the distance of vegetation from powerlines using stereo vision " ISPRS Journal of Photogrammetry & Remote Sensing **60**(4): 269-283.

Whelan, P. F. and O. Ghita (2009). Color texture analysis. Handbook of texture analysis. M. Mirmehdi, X. Xie and J. Suri, Imperial College Press**:** 129-164.

Xie, X. and K.-M. Lam (2006). "Gabor-based kernel PCA with doubly nonlinear mapping for face recognition with a single face image." IEEE Transactions on Image Processing **15**(9).

Yan, G., C. Li, G. Zhou, W. Zhang and X. Li (2007). "Automatic extraction of power lines from aerial images." IEEE Geoscience and Remote Sensing Letters **4**(3): 387-391.

Yang, J., J.-y. Yang, D. Zhang and J.-f. Lu (2003). "Feature fusion: parallel strategy vs. serial strategy." Pattern Recognition **36**: 1369-1381.

Zhang, L., Y. Zhao, B. Huang and P. Li (2008). "Texture feature fusion with neighborhood oscillating tabu search for high resolution image." Photogrammetric Engineering & Remote Sensing **74**(12): 1585-1596.